

Energy Management for Hybrid Power Generation Using Solid Oxide Fuel Cell

A. Haseltalab^a, L. van Biert^{a*}, B.T.W. Mestemaker^b, R.R. Negenborn^a

^a*Delft University of Technology, The Netherlands;*

^b*Royal IHC, The Netherlands*

*Corresponding author. Email: l.vanbiert@tudelft.nl

Synopsis

The shipping industry is facing increasing requirements to decrease its environmental footprints. This challenge is being addressed through the use of alternative fuels and adoption of novel energy sources in advanced power and propulsion systems. In this paper, an energy management approach is proposed to determine the optimal split between different energy sources of a vessel with hybrid power generation. The power and propulsion system of the vessel consists of a gas engine-generator set and a solid oxide fuel cell, both fed with liquefied natural gas, and a battery. Specific fuel consumption curves and transient capabilities of the engine and fuel cell are used to determine the optimal split and the battery is used to deal with the fast load transients during heavy operations and also providing power during low power demanding activities. The performance of the proposed approach is evaluated for a dredging vessel with a DC power and propulsion system and compared to a benchmark vessel powered by gas engine-generator sets only. The results indicate a 16.5% reduction in fuel consumption compared to a benchmark non-hybrid power system and conventional power management.

Keywords: Solid oxide fuel cell; Battery; Hybrid power generation; DC power and propulsion system; Energy management; Liquefied natural gas.

1 Introduction

Increasingly stringent regulations on emissions of hazardous air pollutants, such as sulphur oxides, nitrogen oxides (NO_x) and particulate matter as well as greenhouse gases, in shipping drive the adoption of alternative fuels and clean energy conversion technologies [6]. Liquefied natural gas (LNG) is emerging as a transition fuel towards clean, renewable alternatives, allowing immediate reduction of some of the fuel bound emissions from shipping, in particular sulfur and particulate matter, as well as NO_x formation when burned lean [7].

However, natural gas engines are not on par with diesel generators when it comes to load following capabilities [8]. When pure gas engines are used, the big load steps encountered when dredging may cause the engines to cut off, disrupting the operation and potentially damaging the system. Dual fuel engines can prevent power loss by switching to diesel mode, but this is an undesired solution. Hybridisation with auxiliary energy storage, such as flywheels or batteries, may offer a better solution, as was demonstrated by Mestemaker et al. [17] previously.

Solid oxide fuel cells (SOFCs) provide an alternative to convert natural gas into electricity for power and propulsion systems [19]. The fuel is converted through an electrochemical reaction, thus omitting the high temperature combustion process. As a result, electrical efficiencies can be as high as 65% based on the lower heating value (LHV), and emissions of methane, volatile organic compounds and NO_x are practically zero [25]. Despite the prospects of low specific fuel consumption and virtually no hazardous air pollutant emissions, SOFCs are only applied in niche markets such as combined heat and power and distributed power generation for remote businesses and datacenters with no access to a reliable electricity grid [30].

Maritime application of SOFCs has been studied in various research and demonstration projects. An SOFC-gas turbine combined system generating electricity, heat and cooling was studied in the FELICITAS project [24]. In the METHAPU project, a 20 kW methanol-fuelled SOFC system was demonstrated on the RoRo carrier Wallenius Wilhelmsen [1, 21]. This demonstration was complemented with a life cycle analysis and a conceptual design of an offshore supply vessel [23, 9]. A diesel-fuelled SOFC system was developed in the SchIBZ project, demonstrating efficiencies up to 55% on the MS Forester [18, 15]. This study is part of the GasDrive project, aiming to minimise emissions and energy losses at sea with LNG, combined prime movers, underwater exhausts and nano hull materials [27].

In this paper, the performance of an SOFC power plant combined with a gas engine-generator set and a battery is studied. A novel energy management approach is proposed which instantaneously determines the optimal split between different power sources is studied. A DC microgrid is used for energy distribution and LNG is considered as the primary fuel for both the engine and the SOFC. Specific fuel consumption (SFC) curves of a gas engine and SOFC are used such that quadratic programming approaches can be adopted to solve the optimisation problem, while respecting the transient limitations of the power sources, especially of the SOFC module.

The performance of an all-electric DC power and propulsion (PPS) system with instantaneous energy management is evaluated in a case study of a cutter suction dredger (CSD). The dredging operating profiles are provided by Royal IHC, while the component models and their relevant parameters are provided by Damen Schelde Naval Shipbuilding and Royal IHC. The SOFC is designed to cover the base load required during dredging, while the gas engine-generator set is used to follow large load fluctuations. Since the load fluctuations imposed by dredging

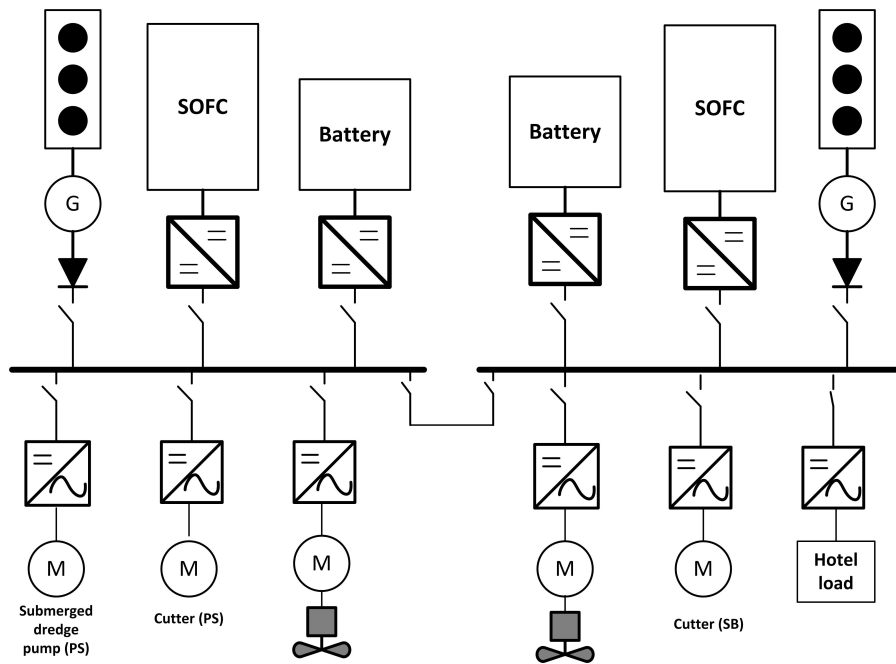


Figure 1: DC PPS of a dredging vessel with hybrid power generation.

operations are typically too fast for a pure gas engine, a battery is used as well for peak shaving and assisting the engine to address fast transients.

2 System description

In this section, the DC PPS with hybrid power generation is discussed and a mathematical model is given for its major components.

2.1 Power and propulsion system architecture

A DC PPS architecture is selected for this study, since due to advances in the domain of semiconductors it is perceived as one of the most efficient architectures [29]. The studied DC PPS architecture is shown in Figure 1. Several advantages of DC-PPS are the possibility for optimal engine loading, variable diesel engine speed, and fuel efficiency, which make this PPS suitable for ships with different operational profiles. Moreover, an increase of flexibility in the design stage and a decrease in the number of converting stages are among advantages of DC on-board microgrids [28, 10]. As a result, DC-PPS can be a proper power system candidate for a wide range of vessels.

In an all-electric DC PPS, the relationship between the energy sources and propulsive and non-propulsive loads are established through a DC microgrid. In Figure 1 a gas engine-generator, an SOFC, and a battery are used on each side of the PPS as energy suppliers, and dredging pumps and cutters in parallel with propulsive induction machines are the major loads.

2.2 Component models

In this section a mathematical model is given for different major components of the DC PPS. For the model of synchronous generator, converters, rectifier, and the DC-link the reader is referred to [13].

2.2.1 SOFC

A model is developed to calculate the current-voltage characteristics, fuel consumption for different loads and transient response of a typical SOFC system with internal reforming of natural gas. Such systems are described extensively in literature, for example by Ahmed et al. [4] and van Biert et al. [26]. The modelling equations are formulated such that the main dependencies are captured correctly, while omitting detailed simulation of electro-chemistry, thermal management and the power consumption of balance of plant components.

The electric power produced by the SOFC stack is calculated from:

$$P_{stack} = U_{stack} I_{stack} = U_{cell} n_{cell} I_{stack}, \quad (1)$$

where U_{cell} the voltage produced by a single cell and n_{cell} the number of cells connected in series in the stack. Assuming that the stack is operated in the region where the internal losses are dominated by an equivalent ohmic resistance. R_{eq} , the single cell voltage is calculated from [22]:

$$U_{cell} = U_{OCV}^* - I_{stack}R_{eq} \quad (2)$$

U_{OCV}^* is a virtual open circuit voltage. The actual open circuit voltage would be higher, but fall rapidly at low loads due to activation losses, as is schematically shown in Figure 2. Since the the SOFC will hardly operate at such low loads, static and activation losses are subtracted from the reversible voltage in the model to account for the losses at low load:

$$U_{OCV}^* = U_{rev} - \Delta U_{OC} \quad (3)$$

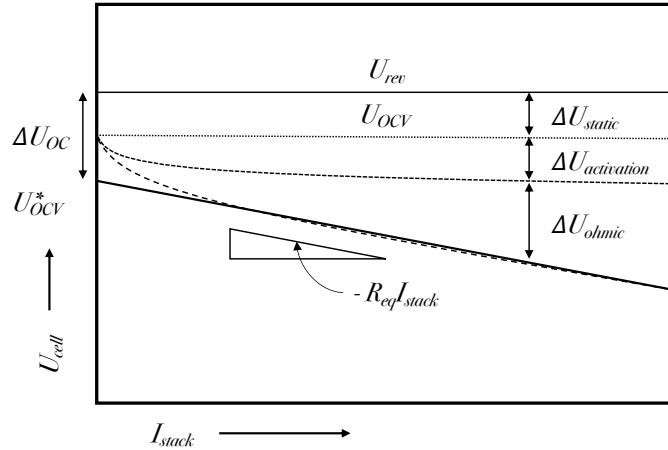


Figure 2: Schematic overview of the simplified method used to estimate the cell potential from the reversible potential R_{rev} , voltage loss at open circuit ΔU_{OC} , stack current I_{stack} and equivalent cell resistance R_{eq} .

The model accounts for both constant and load-dependent power consumption by the auxiliary system components to calculate the actual system power. For any requested SOFC system power, the corresponding stack power thus follows from:

$$P_{stack} = P_{system}(1 + P_{loss,ld}) + P_{loss,c} \quad (4)$$

The stack current required to produce that power can be calculated by solving Equations (1) and (2), giving:

$$I_{stack} = \frac{U_{OCV}^* - \sqrt{(U_{OCV}^*)^2 - 4 * R_{eq} * P_{stack} / n_{cell}}}{2 * R_{eq}} \quad (5)$$

A rate limiter is applied to the stack current to comply with the typical operating limits imposed by SOFC system manufacturers [2]:

$$|I_{stack}|^{max} = \tau_{SOFC} I_{stack}^{rated} \quad (6)$$

The stack current is used to calculate the actual voltage of the stack, as well as the average voltage of a single cell. The single cell voltage can be used to calculate the stack efficiency. The efficiency is defined as:

$$\eta_{stack} = \frac{P_{stack}}{\dot{n}_f \Delta \bar{h}_f} \quad (7)$$

where n_f is the molar fuel flow and $\Delta \bar{h}_f$ the molar lower heating value of the fuel. Since the fuel flow is directly correlated to the stack current, Equation (7) can be shown to be mathematically equivalent to

$$\eta_{stack} = \frac{U_{cell}}{\Delta \bar{h}_f} z F u_f, \quad (8)$$

with z the number of electrons exchanged for complete electrochemical oxidation of the fuel, F Faradays constant and u_f the fuel fraction utilised in the stack, here assumed to be 0.85. The system efficiency, used to calculate the actual SOFC fuel consumption, subsequently follows from:

$$\eta_{system} = \eta_{stack} \frac{P_{system}}{P_{stack}} \quad (9)$$

2.2.2 Gas engines

The gas engine is the primary energy supplier. The engine dynamics can be approximated by nonlinear or linear equations (see, e.g., [16],[12],[11]), depending on the level of accuracy needed. In this paper, a linear model is adopted to accommodate the relationship between the fuel index and produced torque Q_{en} by means of a transfer function as below [5]:

$$\dot{Q}_{en} = -\frac{1}{\tau_{en}}(Q_{en} + K_{en}f_{en}), \quad (10)$$

where K_{en} is the torque constant, f_{en} is the governor setting (i.e., fuel index and flow) and τ_{en} is the torque buildup constant which determines the response speed of the gas engine and is determined by the engine specification and speed. The power generated by the engine is calculated as:

$$P_{en} = \omega_{dg} Q_{en} \quad (11)$$

where ω_{dg} represents the rotational speed.

2.2.3 Battery

A model from [20] is used to simulate the battery dynamics. This is suitable for power and energy management purposes. The State-of-Charge (SoC) of the battery is determined using:

$$S_{oC}(k+1) = S_{oC}(k) - \left(\frac{\eta_i \Delta t}{C_n}\right) i_b, \quad (12)$$

where η_i is the cell Coulombic efficiency, i.e., $\eta_i = 1$ for discharge and $\eta_i \leq 1$ for charge. Parameter C_n is the nominal capacity of the battery, k is the sampling time, Δt is the sampling period, and i_b is the battery current. The battery voltage can be derived as:

$$v_b = O_{CV}(S_{oC}(k)) - r_b i_b, \quad (13)$$

where O_{CV} is the open circuit voltage of the battery and is a function of S_{oC} and r_b is the battery resistance.

3 Proposed Energy Management Approach

The energy management approach is designed to determine the optimal split between different energy sources instantaneously. The optimisation problem is formulated using the SFC of the energy sources. Take

$$S_{FC_{en}}(P_{en}(k)) = a_{en} P_{en}(k) + \frac{c_{en}}{P_{en}(k)} + b_{en} \quad (14)$$

as SFC function of the gas engine in which a_{en} , b_{en} , and c_{en} are constant variables and k is the time constant. Similarly the SFC curve of the SOFC can be defined as:

$$S_{FC_{fc}}(P_{fc}(k)) = a_{fc} P_{fc}(k) + \frac{c_{fc}}{P_{fc}(k)} + b_{fc} \quad (15)$$

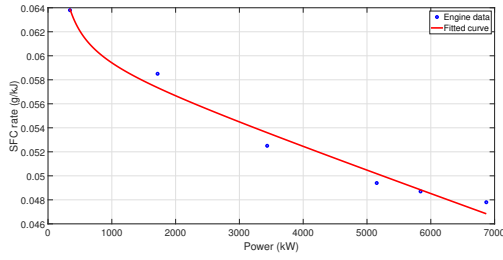
where P_{fc} is the generated power by the SOFC. In case of offshore charging, the penalty for the use of the battery in discharge mode depends on how efficiently the battery can be charged. As a result, this variable is determined by the ship operator and based on the SFC curves of the gas engine and SOFC as well as the battery losses. This variable is estimated based on how much fuel is required to charge the battery. Let us indicate this constant with a_{batt} . The unit of this variable is g/kJ . In Figure 3, the SFC curves of a gas engine and an SOFC is shown. The SFC curve of the engine is estimated based on the data of an existing engine and SFC data of the SOFC is calculated theoretically based on the results in Section 2.2.1.

Using Equations (14) and (15) and the penalty for the battery usage, the overall fuel consumption of the each PPS side in discharge mode, at every sampling time k of the energy management module, can be estimated as:

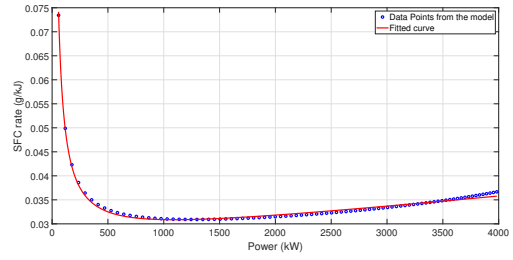
$$f_{cnp}(P_{en}(k), P_{fc}(k), P_{batt}(k)) = a_{en} P_{en}^2(k) + b_{en} P_{en}(k) + c_{en} + a_{fc} P_{fc}^2(k) + b_{fc} P_{fc}(k) + c_{fc} + a_{batt} P_{batt}(k) \quad (16)$$

where P_{batt} is the battery's power. Based on Equation (16), a quadratic optimisation problem can be formulated to determine the optimal split between different energy sources as:

$$\mathbb{P}_{EM} : \min_{P_{en}(k+1), P_{fc}(k+1), P_{batt}(k+1)} J(P_{en}(k+1), P_{fc}(k+1), P_{batt}(k+1)) \quad (17)$$



(a) SFC function of the gas engine (Wärtsilä 6L46DF)[3].



(b) SFC curve of a 4 MW SOFC plant.

Figure 3: SFC curves vs. the engine and the SOFC fuel consumption data.

subject to:

$$\begin{aligned}
 P_{en}(k+1) + P_{fc}(k+1) + P_{batt}(k+1) &= P_{Load}(k) \\
 |\Delta P_{en}(k)| &\leq P_{change_{en}} \\
 |\Delta P_{fc}(k)| &\leq P_{change_{fc}} \\
 P_{min_{en}} &\leq P_{en}(k+1) \leq P_{max_{en}} \\
 P_{min_{fc}} &\leq P_{fc}(k+1) \leq P_{max_{fc}} \\
 P_{min_{batt}} &\leq P_{batt}(k+1) \leq P_{max_{batt}}
 \end{aligned} \tag{18}$$

where

$$J(P_{en}(k+1), P_{fc}(k+1), P_{batt}(k+1)) = a_{en}P_{en}^2(k+1) + b_{en}P_{en}(k+1) + a_{fc}P_{fc}^2(k+1) + b_{fc}P_{fc}(k+1) + a_{batt}P_{batt}(k+1), \tag{19}$$

parameter P_{Load} is the load power measured at the DC-link, $\Delta P_{en}(k) = P_{en}(k+1) - P_{en}(k)$, and $\Delta P_{fc}(k) = P_{fc}(k+1) - P_{fc}(k)$.

A similar optimisation problem can be used for the charge mode in which the constraints on the battery is different. To solve the optimisation problem in Equation (17) quadratic programming approaches can be adopted which leads to a fast response of the energy management module.

If the solutions to the problem \mathbb{P}_{EM} are shown with $P_{en}^*(k+1)$, $P_{fc}^*(k+1)$, and $P_{batt}^*(k+1)$, then the power share of each energy source is calculated as:

$$\begin{aligned}
 \alpha_{en}(k+1) &= \frac{P_{en}^*(k+1)}{P_{en}^*(k+1) + P_{fc}^*(k+1) + P_{batt}^*(k+1)} \\
 \alpha_{fc}(k+1) &= \frac{P_{fc}^*(k+1)}{P_{en}^*(k+1) + P_{fc}^*(k+1) + P_{batt}^*(k+1)}.
 \end{aligned} \tag{20}$$

For the discharge mode:

$$\alpha_{batt}(k+1) = \frac{P_{batt}^*(k+1)}{P_{en}^*(k+1) + P_{fc}^*(k+1) + P_{batt}^*(k+1)}, \tag{21}$$

and for the charge mode $P_{batt}^*(k+1)$ is part of the load power.

4 Simulation Experiments

In this section, the performance of the DC PPS with hybrid power generation in combination with the proposed energy management approach is evaluated. Operating profiles of a Royal IHC dredging vessel are considered for the evaluation. The overall power generation capability of the vessel is 25740 kW, in which each side of the PPS has a power generating capacity of 12870 kW. The performance of the energy management approach is evaluated using two operating profiles of a cutter suction dredger; a 3.5 hrs dredging in rock and a 4.7 hrs dredging in sand. The simulation is carried out two times for each profile with initial battery SoCs of 18% and 92% respectively.

The benchmark vessel is powered with gas engine-generator sets only, providing a the required total power of 25740 kW. For the hybrid concept, the rated power of the gas engine-generator and the SOFC is 6870 kW and 4000 kW respectively, and the battery power capacity is 2000 kW. The reader is referred to [14, 17] for the validation of the different electrical component models. The PPS component parameters are presented in the Appendix.

Figure 4 shows simulation results for 3.5 hrs dredging in rock. Figure 4a shows the load power measured at the DC-link which fluctuates heavily during the operation. The DC-link voltage which is an indication of stability is

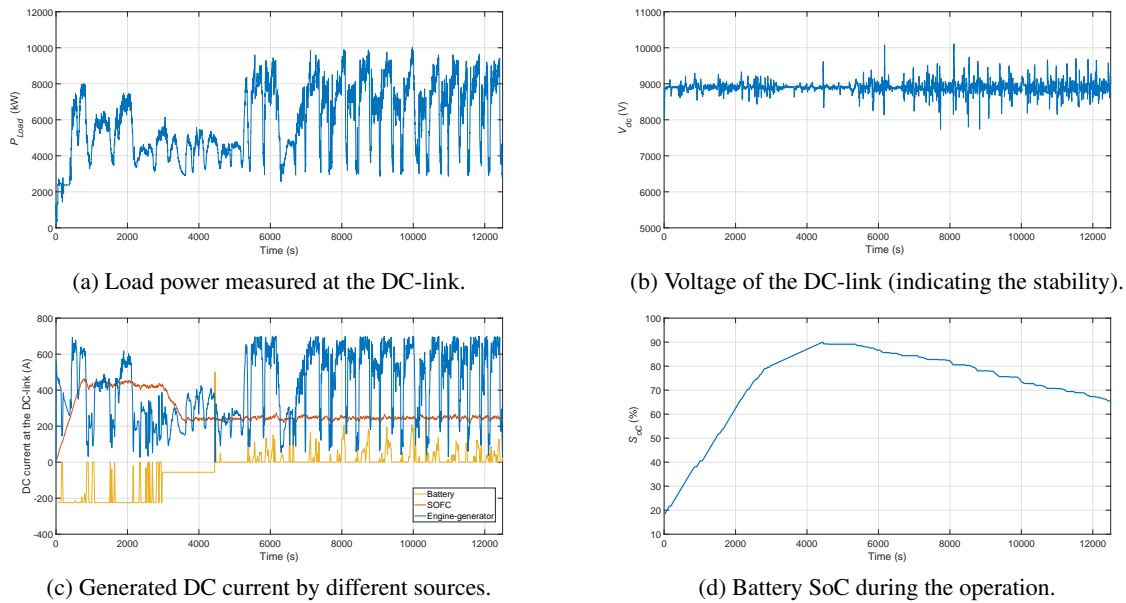


Figure 4: Simulation results of 3.5 hrs dredging in rock with the battery on initial charge mode.

Table 1: Energy delivered and fuel consumption for rock and sand cutting with hybrid power generation using the energy management approach, compared to a non-hybrid conventional benchmark. The hybrid system is evaluated for two different initial battery SoCs.

Simulation scenario	Initial SoC (%)	Energy delivered (kWh)			Fuel consumption (kg)		SFC (g/kWh)
		Battery	Gas engine	SOFC	Gas engine	SOFC	
hybrid-rock	18	-972	13240	7417	2436	867	167.8
hybrid-rock	92	575	12840	6509	2368	746.8	156.3
benchmark-rock	-	-	10560 × 2	-	2030 × 2	-	192.3
hybrid-sand	18	-1001	15360	9737	2875	1135.2	166.4
hybrid-sand	92	559.2	14950	8816	2803	1010.9	156.7
benchmark-sand	-	-	12960 × 2	-	2529 × 2	-	195.3

shown in Figure 4b. As a result of load fluctuations, the DC-link voltage also fluctuates. However, it stays around its nominal point which indicates that the proposed energy management approach properly allocates the loads. The DC-link current generated by each power source is included in 4c and the battery SoC is shown in 4d. The battery is charged first and then discharged during the dredging operation.

The simulation results of 4.7 hrs dredging in sand is included in Figure 5. The power shares for different energy sources over time, determined by the energy management approach, is shown in Figure 5b. Figure 5 shows the fuel consumption rate of the SOFC and the gas engine, and the power generated by each energy source is shown in Figure 5d. In both Figures 4 and 5 it can be seen that a base load is provided by the SOFC, while transients are followed by the battery and the gas engine.

Table 1 summarises the overall results for the load profiles in Figure 4a and Figure 5a. Each case is carried out for two different battery modes. The results are compared to a case where only engine-generator sets are installed to compare the fuel efficiency to a conventional PPS. The results indicate that the fuel consumption is significantly decreased with the hybrid PPS. The SFC of the hybrid PPS with the proposed energy management approach is 161.8 g/kWh on average, while it is 193.8 g/kWh for the benchmark system with gas engine-generator sets only. This indicates that the proposed approach can reduce the fuel consumption with 16.5% compared to the benchmark system with gas engine-generator sets only.

5 Conclusions

In this paper, an energy management approach is proposed for a novel power and propulsion system (PPS) with hybrid power generation which consists of a gas engine, a solid oxide fuel cell (SOFC), and a battery. The energy management approach is designed using the specific fuel consumption curve of the gas engine and the SOFC. The optimisation problem of the energy management is formulated such that the quadratic programming approaches

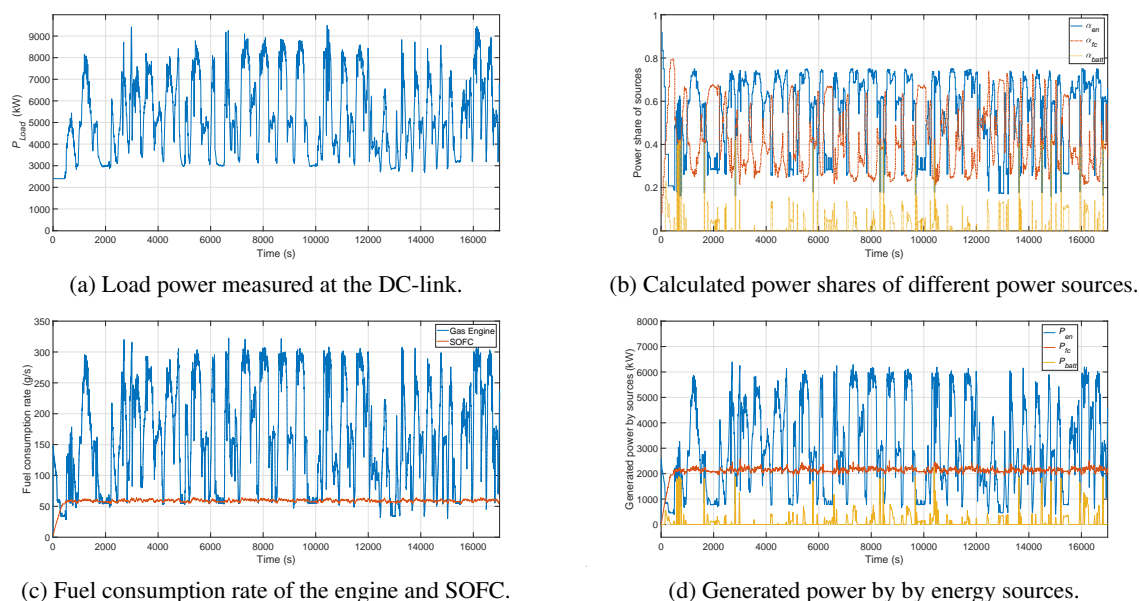


Figure 5: Simulation results of 4.7 hrs dredging in sand with the battery on initial discharge mode.

can be used to solve the optimisation problem. A dredging vessel of Royal IHC is used as the case study with two cutter suction dredging operating profiles in rock and sand. The results indicate a 16.5% reduction in fuel consumption compared to a benchmark non-hybrid power system and conventional power management.

Acknowledgement

This research is supported by the project “GasDrive: Minimizing emissions and energy losses at sea with LNG combined prime movers, underwater exhausts and nano hull materials” (project 14504) of the Netherlands Organisation for Scientific Research (NWO), domain Applied and Engineering Sciences (TTW), the project “NoMES: Novel and Minimized Emissions Shipping” of the Nederland Maritiem Land (NML) and the Researchlab Autonomous Shipping (RAS) of Delft University of Technology.

References

- [1] METHAPU prototypes methanol SOFC for ships. *Fuel Cells Bulletin*, 2008(5):4 – 5, 2008.
- [2] Staxera GmbH (D). Technical Documentation Integrated Stack Module (ISM). Technical report available at the web site http://www.fuelcellmarkets.com/content/images/articles/00864_AS_Dokumentation_ISM.pdf, 2010. Accessed: 2018-10-09.
- [3] Wärtsilä Engines & Generating sets. Brochure, 2016.
- [4] Khaliq Ahmed and Karl Föger. Perspectives in solid oxide fuel cell-based microcombined heat and power systems. *Journal of Electrochemical Energy Conversion and Storage*, 14(3):031005, 2017.
- [5] M. Blanke and J.S. Andersen. *On Dynamics of Large Two Stroke Diesel Engines: New Results from Identification*. 1984.
- [6] Selma Brynolf, Maria Taljegard, Maria Grahn, and Julia Hansson. Electrofuels for the transport sector: a review of production costs. *Renewable and Sustainable Energy Reviews*, 81:1887–1905, 2018.
- [7] Fabio Burel, Rodolfo Taccani, and Nicola Zuliani. Improving sustainability of maritime transport through utilization of Liquefied Natural Gas (LNG) for propulsion. *Energy*, 57:412–420, 2013.
- [8] Cimac workgroup “Gas engines”. Position paper: transient response behaviour of gas engines. CIMAC, 2011.
- [9] Maria C Díaz-de Baldasano, Francisco J Mateos, Luis R Núñez-Rivas, and Teresa J Leo. Conceptual design of offshore platform supply vessel based on hybrid diesel generator-fuel cell power plant. *Applied Energy*, 116:91–100, 2014.
- [10] R.D. Geertsma, R.R. Negenborn, K. Visser, and J.J. Hopman. Design and control of hybrid power and propulsion systems for smart ships: A review of developments. *Applied Energy*, 194:30 – 54, 2017.
- [11] R.D. Geertsma, R.R. Negenborn, K. Visser, M.A. Loonstijn, and J.J. Hopman. Pitch control for ships with diesel mechanical and hybrid propulsion: Modelling, validation and performance quantification. *Applied Energy*, 206:1609 – 1631, 2017.

- [12] PJM; Stapersma D Grimmeliuss, HT; Schulten. The use of diesel engine simulation models in ship propulsion plant design and operation. In *CIMAC, 2007*, 2007.
- [13] Ali Haseltalab. *Control for Autonomous All-Electric Ships*. PhD thesis, Delft University of Technology, 2019.
- [14] Ali Haseltalab and Rudy R Negenborn. Model predictive maneuvering control and energy management for all-electric autonomous ships. *Applied Energy*, 251:113308, 2019.
- [15] Gerardo Valadez Huerta, Johanan Álvarez Jordán, Tobias Marquardt, Michael Dragon, Keno Leites, and Stephan Kabelac. Exergy analysis of the diesel pre-reforming SOFC-system with anode off-gas recycling in the SchIBZ project. Part II: System exergetic evaluation. *International Journal of Hydrogen Energy*, 44(21):10916–10924, 2019.
- [16] Roozbeh Izadi-Zamanabadi and Mogens Blanke. A ship propulsion system as a benchmark for fault-tolerant control. *Control Engineering Practice*, 7(2):227 – 239, 1999.
- [17] B T W Mestemaker, M B Goncalves Castro, H N van den Heuvel, and K Visser. Dynamic simulation of a vessel drive system with dual fuel engines and energy storage. *Energy*, page 116792, 2019.
- [18] Pedro Nehter, Barbara Wildrath, Ansgar Bauschulte, and Keno Leites. Diesel based SOFC demonstrator for maritime applications. *ECS Transactions*, 78(1):171–180, 2017.
- [19] Richard Payne, Jonathan Love, and Michael Kah. Generating electricity at 60% electrical efficiency from 1-2 kWe SOFC products. *ECS Transactions*, 25(2):231–239, 2009.
- [20] Gregory L. Plett. Extended kalman filtering for battery management systems of lipb-based hev battery packs: Part 1. background. *Journal of Power Sources*, 134(2):252 – 261, 2004.
- [21] Juergen Rechberger, Richard Schauerl, John Bogild Hansen, and Peter K Larsen. Development of a methanol SOFC APU demonstration system. *ECS Transactions*, 25(2):1085–1092, 2009.
- [22] AA Salam, MA Hannan, and Azah Mohamed. Dynamic modeling and simulation of solid oxide fuel cell system. In *2008 IEEE 2nd International Power and Energy Conference*, pages 813–818. IEEE, 2008.
- [23] C Strazza, A Del Borghi, P Costamagna, A Traverso, and M Santin. Comparative LCA of methanol-fuelled SOFCs as auxiliary power systems on-board ships. *Applied Energy*, 87(5):1670–1678, 2010.
- [24] Lawrence K C Tse, Steven Wilkins, and Ricardo F Martinez-Botas. Dynamic modelling of a SOFC-GT hybrid system for transport applications. In *European Ele-Drive Conference Brussels, Belgium*, 2007.
- [25] L van Biert, M Godjevac, K Visser, and P V Aravind. A review of fuel cell systems for maritime applications. *Journal of Power Sources*, 327:345–364, 2016.
- [26] L van Biert, K Visser, and PV Aravind. A comparison of steam reforming concepts in solid oxide fuel cell systems. *Applied Energy*, 264:114748, 2020.
- [27] Lindert van Biert. *Solid oxide fuel cells for ships: System integration concepts with reforming and thermal cycles*. PhD thesis, Delft University of Technology, 2020.
- [28] B. Zahedi and L.E. Norum. Modeling and simulation of all-electric ships with low-voltage dc hybrid power systems. *Power Electronics, IEEE Transactions on*, 28(10):4525–4537, Oct 2013.
- [29] Bijan Zahedi, Lars E. Norum, and Kristine B. Ludvigsen. Optimized efficiency of all-electric ships by dc hybrid power systems. *Journal of Power Sources*, 255:341 – 354, 2014.
- [30] Li Zhao, Jacob Brouwer, Sean James, Eric Peterson, Di Wang, and Jie Liu. Fuel cell powered data centers: In-rack dc generation. *ECS Transactions*, 71(1):131, 2016.

Appendix

- **SOFC:** $U_{rev} = 1.039$ V, $\Delta U_{OC} = 0.1$ V, $n_{cells} = 1200$, $P_{loss,ld} = 0.025$, $P_{loss,c} = 0.025$, $R_{eq} = 0.0478$ Ω , $\Delta \bar{h}_f = 789.2$ kJ mol⁻¹, $z = 8$, $F = 96485$ C mol⁻¹, $u_f = 0.85$, $U_{cell}^{rated} = 0.7$ V, $\tau_{SOFC} = \frac{1}{900}$ s⁻¹.
- **Gas Engine:** $K_{en} = 109340$, six cylinders, 6.8 MW, diesel-generator gear ratio: $\frac{1}{6}$.
- **Synchronous generator I:** 6.150 MW, 6600 v, 60 Hz, 10 poles, $H = 0.71$, $r_s = 0.0363$, $r_{fd} = 0.2$, $r_{kd} = 0.722$, $r_{kq} = 0.1072$, $L_d = 0.0323$, $L_{md} = 0.0305$, $L_{kd} = 0.0320$, $L_{fd} = 0.4820$, $L_q = 0.0163$, $L_{mq} = 0.0144$ and $L_{kq} = 0.0163$. Resistance values are in ohm and inductance values are in Henry.
- **Synchronous generator II:** 3.456 MW, 6600 v, 60 Hz, 10 poles, $H = 0.56$, $r_s = 0.0601$, $r_{fd} = 0.177$, $r_{kd} = 1.5049$, $r_{kq} = 0.1726$, $L_d = 0.05768$, $L_{md} = 0.05407$, $L_{kd} = 0.06125$, $L_{fd} = 0.3204$, $L_q = 0.02702$, $L_{mq} = 0.0144$ and $L_{kq} = 0.02341$. Resistance values are in ohm and inductance values are in Henry.
- **Rectifier:** Six-pulse rectifier, efficiency factor: 98.1%.
- **DC-link:** $C = 1$ F.
- **Bidirectional Converter-battery:** $L = 0.0005$ H, $v_b = 500$ V, $r_b = 0.0125$.